

## INFLUENCE OF GROWTH AND STRUCTURE ON THE MAGNETISM OF EPITAXIAL COBALT FILMS ON CU(001)

C.M. Schneider<sup>1</sup>, A.K. Schmid<sup>2</sup>, P. Schuster<sup>2</sup>, H.P. Oepen<sup>3</sup>  
and J. Kirschner<sup>1</sup>

<sup>1</sup> MPI für Mikrostrukturphysik, Weinberg 2, O-4050 Halle/Saale

<sup>2</sup> Inst. f. Experimentalphysik, FU Berlin, Arnimallee 14  
W-1000 Berlin 33

<sup>3</sup> IGV, Forschungszentrum Jülich GmbH, Postfach 1913  
W-5170 Jülich

### INTRODUCTION

Artificially layered materials and ultrathin films of ferromagnetic substances currently receive considerable interest in materials science. These systems often show novel magnetic properties which differ dramatically from those of the corresponding bulk ferromagnets, e.g., unexpected magnetic anisotropies or surprisingly low Curie temperatures. Research in this field is stimulated by both scientific curiosity and potential applications in magnetic storage and sensor technology. A successful development of new storage devices and technologies requires a fundamental knowledge of the underlying physical mechanisms, in order to be able to deliberately modify the magnetic properties of a given material or system.

Understanding the magnetic properties turns out to be difficult, since the altered magnetic behavior of films in the monolayer regime must generally be attributed to more than one physical mechanism. Although some of the effects appear due to the reduced dimensionality, it has been realized that crystalline structure and peculiarities in the epitaxial growth process of ultrathin films play a crucial role. This is particularly important in the case of layers built up from metastable crystalline phases, such as face centered cubic iron or cobalt. A thorough understanding of the magnetic properties of epitaxial systems thus requires a broad data base which must include structural aspects and a precise characterization of the growth process in its various stages, as well as the influence of the growth conditions. This "wide band" approach promises new and yet unprecedented insight into the links between structure, topography, morphology and magnetic behavior. As a welcome side aspect, one may expect such an approach to facilitate the comparison of results from different groups on the same system, thus helping to reduce the number of possible inconsistencies. In

the following we report on our investigations and results on ultrathin fcc-cobalt films on Cu(001) substrates.

## EXPERIMENTAL METHODS AND CRYSTAL PREPARATION

In order to analyze the interrelations between growth, crystalline structure, magnetism and electronic states, we characterized the model system cobalt on Cu(001) by a number of different techniques. We employed in-situ diffraction methods (Low Energy Electron Diffraction, Medium Energy Electron Diffraction) in combination with Auger electron spectroscopy, to monitor the epitaxial growth and to determine precisely the film thickness. Conclusions on the crystalline structure are based on the interpretation of LEED patterns and the analysis of  $I(E)$  curves for several diffracted beams. In addition, the surface topology of the substrate and the films has been investigated by real space imaging techniques (Scanning Tunneling Microscopy). The Surface Magneto Optical Kerr effect was employed to study the macroscopic magnetic properties on the basis of hysteresis loops. The electronic structure of the Cu substrate and the Co films has been investigated by means of spin-resolved photoelectron spectroscopy using circularly polarized synchrotron radiation. This gave a detailed insight into the films' electronic structure and the hybridization of film and substrate electronic states. The magnetic microstructure in the Co films has been characterized by imaging magnetic domains with a scanning electron microscope with spin polarization analysis (SEMPA).

The disk-shaped samples of 10 to 12 mm diameter were spark-cut from a high quality copper single crystal and mechanically polished using diamond paste. The crystals were characterized by a mosaic spread of less than  $0.1^\circ$ , the surface normal being within  $0.2^\circ$  along the (001) crystalline axis. After insertion into the ultrahigh vacuum, the surface was prepared by cyclic sputtering and annealing. A well-defined sharp LEED pattern could be observed already after a few cycles, but these surfaces still contained a certain amount of sulphur and carbon and showed a large number of small terraces (size of the order of 100 Å), as judged by the STM. Uncontaminated surfaces with large atomically flat surfaces (average size about 2000 Å) were obtained only after a total cycling time of about 100 hours.

## GROWTH OF CO ON CU: RECIPROCAL VS. REAL SPACE APPROACHES

During the deposition of Co onto the Cu(001) substrate, the diffracted beams in a MEED experiment show pronounced intensity oscillations over a wide range of substrate temperatures and deposition rates<sup>1</sup>. An example is given in figure 1a for the intensity variation of the specular beam at room temperature growth. This result may be routinely achieved only on carefully cleaned and annealed copper substrates. The following conclusions can be drawn from this curve. First, the presence of MEED intensity oscillations indicates a nearly perfect layer-by-layer growth of Co on Cu(001). Secondly, the film thickness can be evaluated from the number of periods, since each relative intensity maximum is usually interpreted as the completion of a monoatomic layer. The method there-

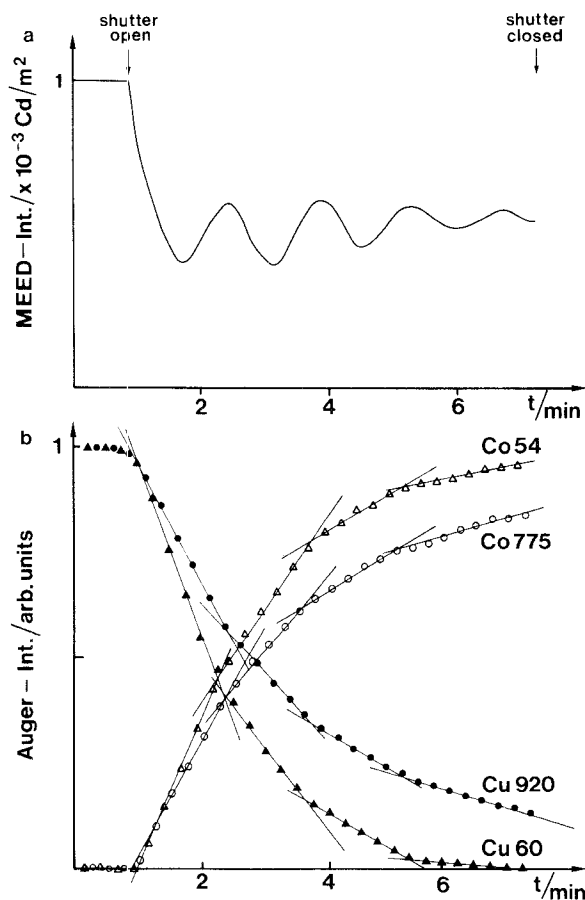


**Fig. 1.** Evolution of the MEED specular intensity (a), and the Auger lines of Co (54 and 775 eV) and Cu (60 and 920 eV) (b). The data have been recorded simultaneously.

fore yields a direct thickness calibration in units of a monolayer (ML). At room temperature, up to several tens of periods in the oscillations have been observed, indicating that rather thick films of fcc cobalt may be grown<sup>2</sup>.

The growth mode is often deduced from the Auger signal vs. deposition time curves. A layer-by-layer growth is concluded if these  $I(t)$  curves can be fitted by a series of straight lines. Each intersection between neighboring lines then marks the completion of a monolayer. This is indeed found in Co/Cu(100) for the Auger lines of cobalt and copper (fig. 1b). It is instructive to compare the results from AES and MEED investigations. This can be done best by performing an experiment, which simultaneously measures the intensity of the diffracted MEED beams and the Auger electrons excited by the primary electrons. The procedure gives a direct correlation between the MEED oscillations and the behavior of the Auger intensities without the ambiguity introduced by different samples. This is actually the way the data in figure 1 have been taken. The direct comparison shows that each maximum in the MEED intensity curve closely corresponds to a

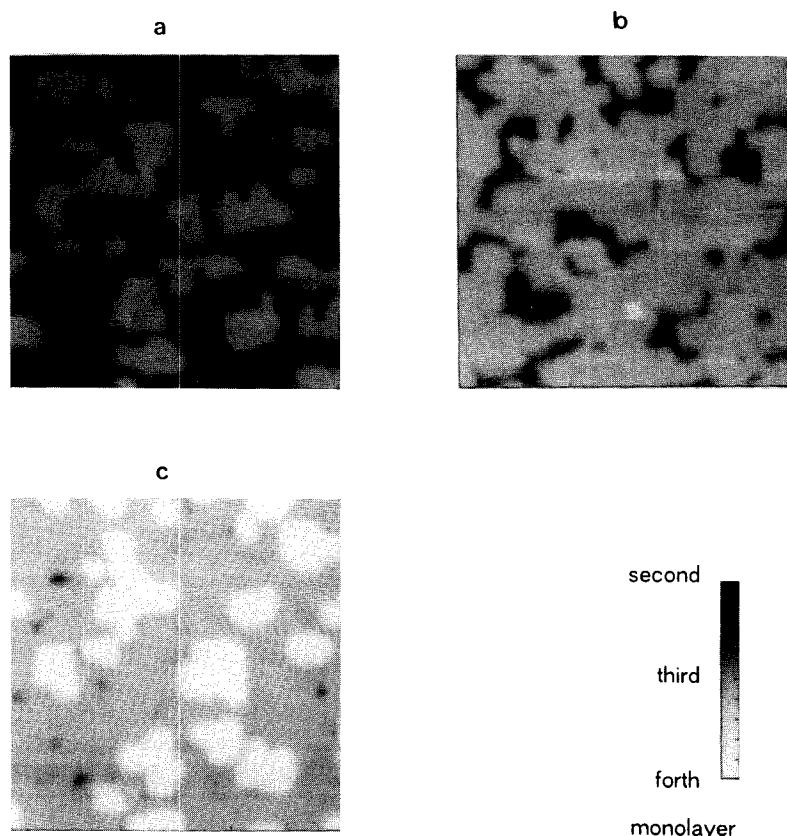


**Fig. 2.** STM micrographs of the growth of Co on Cu(100) subsequently taken from the same spot of the sample surface at coverages of 2.5 (a), 2.9 (b) and 3.3 monolayers. Scale:  $30 \times 30$  nm

kink in the Auger uptake curves. Thus both methods independently and in combination yield the same result and confirm essentially a layer growth of Co on Cu.

A closer inspection of the MEED intensity oscillations, however, suggests that some deviations from the ideal layer-by-layer growth mode must be present. First, after depositing Co, the average intensity of the diffracted beam drops significantly and never comes back to the initial value of the clean Cu surface. Secondly, the oscillations follow a sinusoidal curve rather than a sequence of parabolas expected for the ideal case<sup>3</sup>. These findings can be interpreted by assuming the film to accumulate a certain amount of defects during growth. Further studies showed the average intensity level to be higher during deposition at elevated temperatures up to 450 K, indicating less defects and slightly better growth conditions. Kinetic processes, i.e., surface diffusion, clearly influence the quality of film growth in the Co/Cu system. If only kinetic arguments are considered, a sufficiently high substrate temperature and thus a high adatom mobility should promote the nearly ideal case of a step-flow growth, as seen for

example in the homoepitaxy of copper<sup>4</sup>. The onset of interdiffusion in the Co/Cu system at about 500 K unfortunately sets narrow limits to the choice of substrate temperatures in the growth of Co overlayers.

In order to characterize the role of defects and film topography in more detail we performed in situ STM studies at room temperature. For this purpose, sequences of images were recorded from the same section of the surface after subsequent Co depositions and compared. Figure 2 gives a set of images taken on a  $30 \times 30$  nm scale for Co coverages of 2.5, 2.9 and 3.3 ML. Three discrete height levels corresponding to the second, third and fourth monolayer are transposed into a gray scale. The vertical distance of the neighboring height levels has been determined to 1.8 Å, which agrees with the interlayer distance of fcc-Co. This results justifies the designation "monolayer" for the discrete levels observed in the STM images. Furthermore, it independently confirms the assumption of the model of layer growth, that the islands during growth should have monolayer height. Starting with the 2.5 ML image, one notices an almost closed 2 ML level with very little defects, which is half-covered by islands of the third monolayer. At a coverage of 2.9 ML, the islands have grown in size and most of them have coalesced, but the 3 ML level is not yet completely closed. At a coverage of 3.3 ML, islands of the fourth monolayer have formed, but a few holes in the 3 ML level remain. Similar results have been found at higher thicknesses. These observations lead to the conclusion that coverages corresponding to an

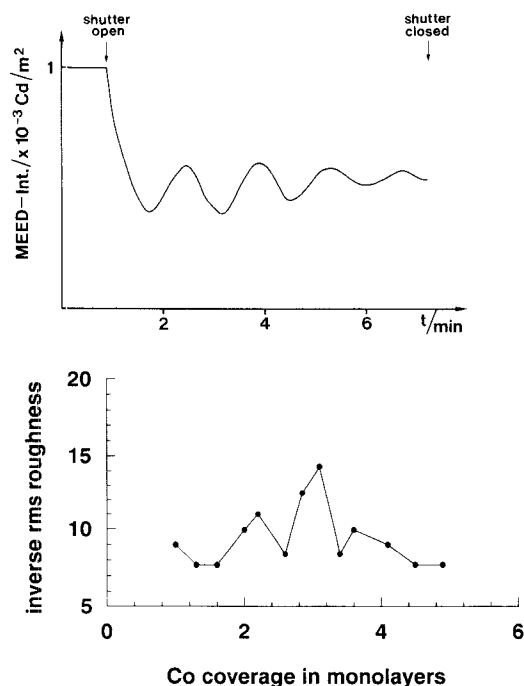


*Fig. 3. Comparison of the inverse rms roughness deduced from a sequence of STM micrographs during the growth of a 5 ML fcc-Co film (b) to the MEED specular intensity (a) reproduced from Fig. 1a*

integral number of layers still contain a certain number of voids and additional islands, resulting in a deviation from the ideal layer-by-layer growth. This interpretation is also consistent with the MEED data. The roughness at integral coverages is confined to the uppermost layer and is of the order of  $\pm 1$  ML.

On the other hand, by analyzing a set of images over a larger range of coverages, one can establish a more quantitative relation between the results of diffraction methods and real space techniques. Evaluating the roughness in each image of the set finally yields a dependence of the surface roughness on the film thickness. This is shown in figure 3a which displays the development of the inverse rms roughness during the growth of a 5 ML film, as obtained by STM. Maxima in this function correspond to minimum roughness and thus the completion of integral layers, minima to half-integral layers. This result is compared to the MEED intensity oscillations reproduced from figure 1a, by scaling the x-axis via Auger calibrations taken for both data sets (see, e.g., the calibration curve in ref. 23). The comparison shows clearly that a reasonable agreement between minima in the surface roughness and maxima in the MEED specular intensity exists. The agreement is not perfect, but this should not be expected for two films grown under different circumstances and in different chambers. In conclusion, these STM results independently warrant the interpretation of MEED intensity oscillations in terms of growth induced changes in the surface topography. Based on the picture of a periodically varying surface roughness, MEED experiments can provide a reliable and precise thickness calibration.

#### IDEAL VS. REAL STRUCTURE: THE INFLUENCE OF TETRAGONALITY

The structure of the films can be deduced from electron diffraction experiments. During the growth of the films one notices intensity oscillations in all diffracted beams, but essentially no deterioration of the diffraction pattern. MEED patterns taken before and after Co deposition are practically indistinguishable. Similar observations have been made with LEED. Experiments on the clean Cu substrate and on carefully prepared Co films yield nearly identical  $p(1 \times 1)$  diffraction patterns over a wide range of coverages. Therefore the lateral lattice mesh of the Co overlayer corresponds to that of the Cu substrate. According to this qualitative analysis, cobalt forms rather thick well-ordered pseudomorphic overlayers on the Cu(100) surface. As the films adopt the fcc lattice of the substrate, one stabilizes the metastable fcc crystal structure of cobalt. In bulk cobalt, the stable structure at room temperature is hcp, a phase transition to the fcc lattice occurring at temperatures above 750 K. In Co films on Cu(100), the fcc modification becomes accessible to experiments at and below room temperature.

In a simplified picture of the crystalline structure, the atoms of the first Co layer occupy the four-fold hollow sites in the Cu surface and the adjacent layers adopt the registry of the fcc substrate lattice. This view assumes the same lattices for cobalt and copper. A comparison of the bulk lattice constants of fcc-Co (3.57 Å) and Cu (3.68 Å) shows that this assumption is at least doubtful. On the basis of these bulk values one has to consider a small lattice mismatch. This will give rise to strain in the film, which must be accommodated either by misfit dislocations or structural deviations from the ideal fcc lattice.

A large data set consisting of LEED I(V) curves for various diffracted beams and several film thicknesses has been compared to dynamical LEED calculations<sup>5</sup>. The analysis leads to the conclusion that the films are indeed subject to a

notable tetragonal distortion normal to the film plane. Due to the lattice mismatch, the surface unit cell of the films is slightly expanded, followed by a compression of the interlayer distance normal to the film plane. This distortion is thickness dependent and relaxes with increasing coverage, where the mean interlayer distance approaches the value of 1.74 Å. This is still somewhat smaller than the corresponding interlayer distance of bulk fcc-Co. The above findings are consistent with an earlier LEED study<sup>6</sup>. The conclusions of a tetragonal distortion of the lattice agree nicely with the results of recent EXAFS experiments on fcc-Co films on Cu(100)<sup>7</sup>.

### Electronic States

The majority and minority spin bands of the Co films have been mapped out along the (001) direction by means of spin- and angle-resolved photoemission. The experimental dispersion of the electronic states was compared to fully relativistic bulk band structure calculations for fcc-Cobalt<sup>8</sup>. During the first few monolayers there is a transition from a two-dimensional to a three-dimensional electronic structure, the latter being almost completely established at a thickness of 5ML. The electronic states at this coverage agree well with the theoretical predictions, except for systematic deviations of the minority bands near the

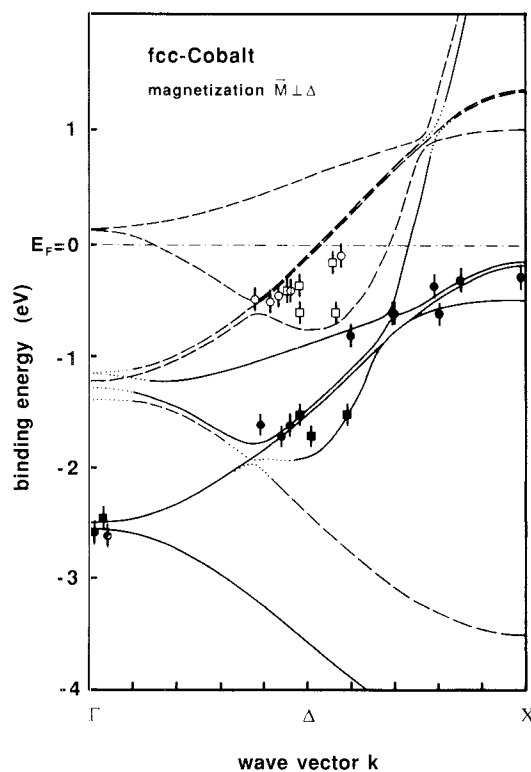


**Fig. 4.** Full relativistic band structure calculation for fcc-Co. Comparison of experimental data for majority (full) and minority states (open symbols).

Fermi level (fig. 4). The experiment finds the minority states at higher binding energies as predicted by the band structure calculation. It should be kept in mind that photoelectron spectroscopy probes the excited state of an electronic system. Therefore a perfect agreement with ground state calculations should not be expected. On the other hand, calculations for simple cubic iron<sup>9</sup> and fcc copper<sup>10</sup> have shown that a tetragonal compression or expansion of the lattice leads to systematic changes in the electronic states as compared to the perfect cubic case. In particular, bands shift their energetic position with respect to the Fermi level. We therefore tentatively attribute the above mentioned deviation to a certain extent to a tetragonal lattice distortion. In fact, the energy position of these minority bands slightly shifts with decreasing Co coverage<sup>11</sup>, thus reflecting thickness dependent changes in the lattice distortion, which are also observed in the LEED experiments mentioned above.

It is interesting to note in this context that Strange et al.'s work on the tetragonal distortion in sc iron<sup>9</sup> showed the magneto-crystalline anisotropy to be strongly influenced by electronic bands in the vicinity of the Fermi level  $E_F$ . A certain band which shifted its energy position and thus the crossing point with  $E_F$  upon the degree of tetragonal distortion, led to a distinct change in the magnetic anisotropy energy. The authors suggested this to be the origin of a flip in the direction of the magnetization from in-plane to out-of-plane. A change of the easy axis of magnetization as a function of the overlayer coverage is indeed known to occur in Fe/Cu(100)<sup>12,13</sup>. Although such a spectacular behavior has not been observed in Co films on Cu(100), a variation of the magnetic anisotropy with the film thickness should not be excluded.

The origin of the magneto-crystalline anisotropy is the spin-orbit interaction in the valence bands, which couples the electron spin to the orbital part of the electronic wave function. Investigations of the electronic structure of ferromagnets often neglect the influence of spin-orbit coupling, because it is considered to be small, at least in the case of 3d metals. This view is contrasted by the results of spin-resolved photoemission experiments from the clean Cu substrate using circularly polarized light<sup>14</sup>. These studies revealed strong spin polarization effects in the 3d bands due to spin-orbit interaction and allowed an experimental determination of the spin-orbit splitting along the (100) direction. It was found to be of the order of 100 meV. One is thus forced to assume that the strength of spin-orbit interaction in the 3d ferromagnets is very similar to the value in Cu. In photoemission experiments from fcc-Co films using circularly polarized light, one indeed observes a phenomenon called magnetic circular dichroism (MCD)<sup>15</sup>. This effect occurs due to the interplay of exchange and spin-orbit interaction and thus directly proved the presence of spin-orbit coupling in the Co 3d valence bands.

### Magnetic Anisotropies

The remanent magnetization of the Co films is always found to lie within the film plane, independent of the film thickness. As revealed by an azimuthal scan in the SMOKE experiments, the films exhibit a pronounced in-plane four-fold anisotropy, the [110] directions being the easy axes of magnetization<sup>16</sup>. This is directly visible in the domain patterns taken with SEMPA, which show only four different directions of the remanent magnetization, which agree with the orthogonal [110] axes<sup>17</sup>. This result is somewhat unexpected, as the easy axis in

fcc materials is known to be the  $\langle 111 \rangle$  direction if the anisotropy constants  $K_1$ ,  $K_2 < 0$ . Negative values for  $K_1$ ,  $K_2$  are known for Ni single crystals and have been reported for fcc Co thick films, too<sup>18</sup>. Within a  $\{100\}$  crystallographic plane, the only low-indexed directions left are  $\langle 110 \rangle$  and  $\langle 100 \rangle$ , with the latter being the energetically least favorable one (hard axis). In a first crude interpretation, the above finding might therefore be attributed to the demagnetizing field, which forces the magnetization into the plane along the easier  $\langle 110 \rangle$  axis. In FMR measurements, however, very strong effective demagnetizing fields  $4\pi M_{\text{eff}}$  of the order of 40 kG have been found<sup>19</sup>. Thus,  $4\pi M_{\text{eff}}$  in ultrathin fcc Co(100) films is about twice as large as the saturation magnetization  $4\pi M_s$ . This gives rise to a negative value of the anisotropy constant  $K_u$ , corresponding to a large perpendicular uniaxial anisotropy with the hard axis along the surface normal. The observed in-plane magnetization in Co(100) films is therefore only partly due to the demagnetizing field. Recalling the discussion in the previous paragraph, this strong uniaxial anisotropy may be a consequence of the tetragonal distortion in the films' structure.

## THE INITIAL STATE OF GROWTH AND THE ONSET OF FERROMAGNETIC ORDER

Monolayer coverages of ferromagnetic materials often show a thickness dependence of the ferromagnetic ordering temperature, which is attributed to the reduced dimensionality in the films. The most striking effect has been reported for fcc cobalt films on Cu(100)<sup>20,21</sup>. According to the results from SMOKE measurements, the Curie temperature  $T_c$  of a 2 ML film is slightly above room temperature. For a single cobalt monolayer, an upper limit of 50 K for  $T_c$  has been found. The thickness dependence of  $T_c$  reported on in ref. 4 is reproduced in Fig. 4 and compared to a recent calculation by P. Bruno<sup>22</sup>. In contrast to the assumptions in the Mermin-Wagner theorem<sup>23</sup>, the calculation considers the influence of long-range dipolar interactions and magnetic anisotropies. It therefore predicts a single monolayer to be ferromagnetically ordered well above 0 K. The reasonable agreement with the experimental data at coverages at and above 2 ML indicates the observed thickness dependence to be partly due to the reduced dimensionality. Below a thickness of 2 ML the agreement becomes worse with decreasing Co coverage. Finally, the experimental values for  $T_c$  of 1 ML films are significantly lower than the theoretical predictions ( $T_{c(\text{theor})} \sim 150$  K). This discrepancy should not be misinterpreted as an experimental evidence for the validity of the Mermin-Wagner theorem, for two reasons. First, with our present experimental set-up we only can give an upper limit for the ordering temperature ( $T_{c(\text{exp})} < 50$  K). The monolayer may therefore show ferromagnetic order below this value. Second, Bruno's calculation does not take into account two important effects, which are immanent to thin film systems. This is, on the one hand, the electronic hybridization between the Co film and the Cu substrate, which should become more important at low film thicknesses. Some indications for such a hybridization are found in spin-resolved photoemission experiments. Furthermore, covering Co films in the monolayer regime with an additional Cu overlayer, i.e. introducing two Co/Cu interfaces, leads to a sizable reduction of the Curie temperature<sup>20,21</sup>. The electronic hybridization obviously tends to lower  $T_c$  and this process gains importance with decreasing film thickness. This effect, however, is not strong enough to explain the extremely low  $T_c$  in the case of the 1 ML film.

The second mechanism may be sought in particularities of the surface topography of the cobalt layers. During the growth of the first monolayer (ML) one indeed observes some irregularities in the MEED and TEAS intensity oscillations, which suggest a deviation from the behavior found at higher coverages<sup>23</sup>. A TEAS analysis of step heights in the monolayer and sub-monolayer regime also indicates differences with respect to thicker layers. These questions have been answered by extensive in-situ STM investigations, which revealed the first Co layer on Cu to grow in a particular manner indeed<sup>24</sup>: contrary to the nearly perfect layer-by-layer growth found at

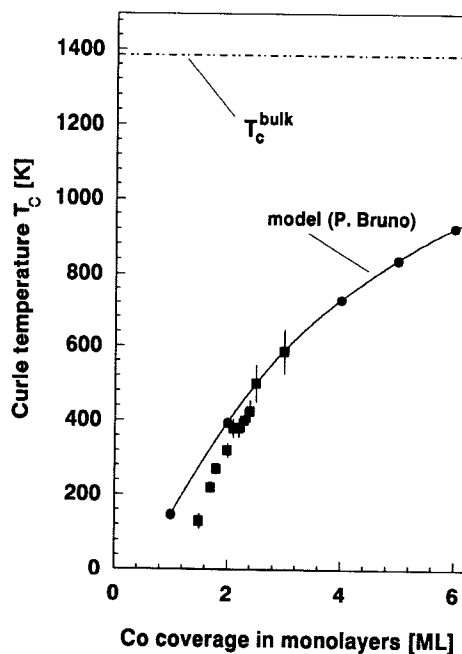
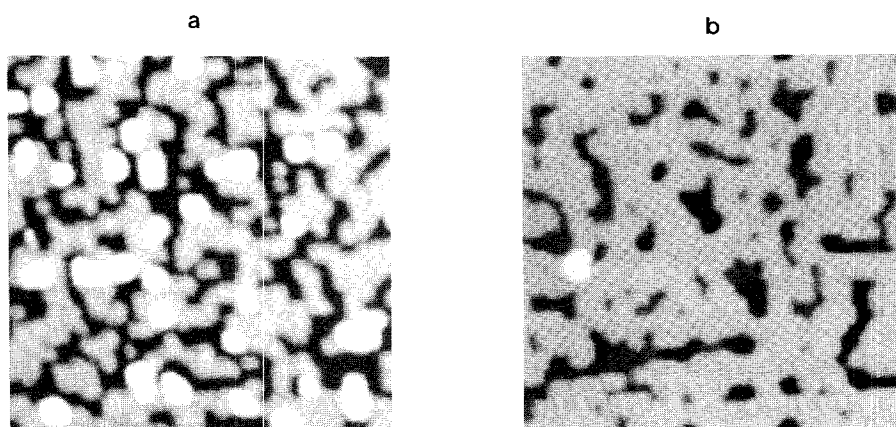


Fig. 5. Thickness dependence of the Curie temperature of fcc-Co films grown on Cu(100). The experimental data points (squares) are compared to a calculation of P. Bruno (circles). The line serves as a guide to the eye.

higher coverages, islands of the second layer nucleate long before the first layer is completed. This is depicted in Fig. 6 showing a comparison of characteristic STM micrographs taken at coverages close to 1 ML (fig. 6a) and 2 ML (fig. 6b). Inspection of fig. 4a proves clearly that the first monolayer does not grow uniformly. About 20% of the substrate surface are yet uncovered, whereas about 20% of the second layer have already formed on top of the first layer islands. As a consequence a Co deposit equivalent to 1 ML yields a significant amount of bilayer islands resulting in a strong deviation from the ideal layer growth. After the deposition of an additional monolayer,

the situation is different (fig. 6b). Nucleation of islands of the third layer does not become significant before the second layer is almost completed. At the equivalent of 2ML and higher, the growth mode obviously changes and becomes more perfect layer-by-layer, the surface roughness at half-integral layers being  $\pm 1\text{ML}$ . These findings clearly point out a difference in the growth mechanisms of Co/Cu vs. Co/Co, as can be expected from thermodynamical considerations<sup>25</sup>.

Coming back to the above question of the discrepancy between the experimental and theoretical  $T_c$  dependence, the results suggest, that the surface topography of the film plays an important role, in particular in the monolayer range. Since the monolayer of Co on Cu(100) contains a rather large fraction of isolated islands, the ferromagnetic coupling may be much weaker than in a filled layer, thus leading to a considerably smaller value of  $T_c$ .



*Fig. 6. STM micrographs taken from the same spot on the sample surface at a coverage of close to 1 ML (a), and after the deposition of an additional monolayer (b). Scale:  $30 \times 30 \text{ nm}$*

#### STEPS AND MAGNETIC ANISOTROPIES

The magnetic properties of a film depend significantly on the structural and topographical quality of the template. Large differences are found, for instance, for films grown on a substrate with large terraces or small terraces. In order to study the influence of atomic steps in a more controlled manner, we prepared a Cu(1113) surface. This surface is vicinal to Cu(001), the surface normal being tilt away from the  $\langle 001 \rangle$  direction by an angle of  $6.2^\circ$  towards the  $\langle 110 \rangle$  axis. Cu(1113) has been subject to recent STM investigations by Frohn et al.<sup>26</sup>. These studies revealed the surface to consist of (001) terraces with an average width of 7 atoms in the  $\langle 110 \rangle$  direction. The terraces are separated by monoatomic steps with the step edges running essentially along  $\{110\}$ .

The growth of Co films on this vicinal surface as seen in MEED experiments proceeds layer-by-layer, but shows a striking difference as compared to the (100) oriented template. The intensity of the specular beam maintained a high level and only very few and weak oscillation periods are visible<sup>27</sup>. This suggests that the growth takes place predominantly via a step flow mechanism. Because of the small width of the terraces, the adatoms can easily reach the next terrace edge, and the step density at the surface remains nearly unaltered. Thus, no major drop in the MEED specular intensity will occur.

The magnetic properties of these Co(1113) films are even more striking. Investigations with SEMPA reveal that only two directions of the remanent magnetization in the domains appear<sup>27</sup>. This is in sharp contrast to the situation in Co(100) films. The magnetization within the domains in Co(1113), and thus the easy axis, is oriented always along the step edges. Despite this surprising difference in the anisotropy, the domain patterns observed in Co(100) and Co(1113) are very similar.

The above SEMPA results have been confirmed by measuring the azimuthal dependence of the hysteresis loops with SMOKE. Results for a 10 ML film are shown in figure 7. An angle  $\Phi = 90^\circ$  ( $0^\circ$ ) corresponds to the external field  $H$  applied parallel (perpendicular) to the step edges. In the case where  $H$  is almost

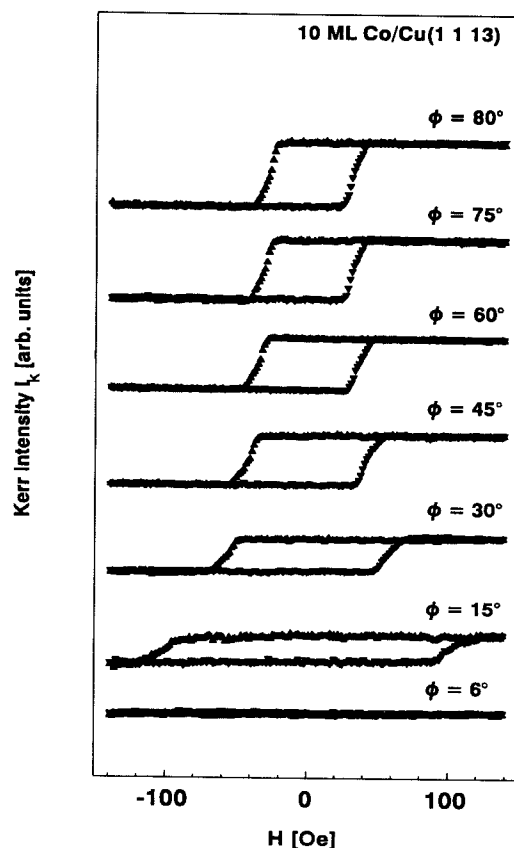


Fig. 7. SMOKE hystereses loops from Cobalt films on Cu(1113) as a function of the azimuthal angle  $\Phi$ .

normal to the steps ( $\Phi = 6^\circ$ ), the coercive field  $H_c$  of the film exceeds a value of 150 G, which is the maximum field we can achieve with the present set-up. The angular variation of the coercive force follows closely a  $\sin(\Phi)$  behavior. This is a consequence of the fact that the magnetization reversal occurs along the easy axis, being induced only if the geometrical projection of the external field along this direction exceeds the easy axis coercive field.

One might be tempted to think of the steps at the surface being responsible for this behavior. In a film of 10 ML thickness, however, the magnetic properties should be bulk-dominated, the surface having only minor influence. It should also be mentioned that very similar  $\Phi$ -dependences have been found for Co coverages between 2 and 10 ML<sup>28</sup>. This suggests that a different mechanism must be employed, which is due to the structural differences of the very films. From the crystallographic point of view, the Co(1113) film has a significantly lower rotational symmetry (two-fold) than the low-indexed (100) surface (four-fold). In fact, one may regard Co(1113) films as a new artificial type of solid with a lowered symmetry, the latter being reflected by the uniaxial magnetic anisotropy. This finding points out a very interesting link between structural symmetries and magnetic anisotropies. Similar observations have been reported for Fe films on vicinal tungsten surfaces<sup>29</sup>. In contrast to the above findings, these systems have the easy axis normal to the step edges. The reason for the different behavior of Fe and Co films is yet unknown. Clearly more work is needed to be able to explain the magnetic properties of these novel systems.

## SUMMARY AND CONCLUDING REMARKS

The above compilation of results gives an overview of the complex interrelations between structure, electronic states and magnetic properties in the model system Co/Cu(100). One is led to the conclusion that details of the crystalline structure and film topography do indeed strongly influence certain magnetic properties, i.e., the anisotropy and ferromagnetic ordering temperature. Since the effects are already very pronounced in single layer films, one must expect an increase in complexity, when going to sandwiches or multilayers. This is not only due to the larger number of interfaces and films involved, but also caused by the appearance of new magnetic effects in these systems, such as oscillatory interlayer coupling and giant magnetoresistance. It can be suspected that discrepancies like the one reported for the absence<sup>30</sup> or presence<sup>31</sup> of the oscillatory interlayer coupling in Co/Cu(111) multilayers, originate from structural or morphological differences in the samples. Clearly, future investigations on magnetic ultrathin film systems must pay attention to both macroscopic and microscopic aspects, in order to yield a better understanding of the magnetic properties.

## ACKNOWLEDGEMENTS

This project has been supported by the Bundesminister für Forschung und Technologie through grant No. 05 413 AXI 03 and the Deutsche Forschungsgemeinschaft through SFB 6. C.M.S., P.S. and J. K. appreciate a fruitful cooperation with the group of R. Miranda at the Universidad Autonoma de Madrid.

## REFERENCES

1. J.J. de Miguel, A. Cebollada, J.M. Gallego, S. Ferrer, R. Miranda, C.M. Schneider, P. Bressler, J. Garbe, K. Bethke, and J. Kirschner, *Surf. Science* **211/212**: 732 (1989)
2. H.P. Oepen, priv. communication
3. B. Poelsema, R. Kunkel, N. Nagel, A.F. Becker, G. Rosenfeld, L.K. Verheij, and G. Comsa, *Appl. Phys. A* **53**: 369 (1991)
4. J.J. de Miguel, A. Cebollada, J. M. Gallego, J. Ferron, and S. Ferrer, *J. Cryst. Growth* **88**: 442 (1988)
5. A. Cebollada et al., see these proceedings
6. A. Clarke, G. Jennings, R.F. Willis, P.J. Rous, and J.B. Pendry, *Surf. Science* **187**: 327 (1987)
7. D. Chandesris et al., see these proceedings
8. C.M. Schneider, P. Schuster, M. Hammond, H. Ebert, J. Noffke, and J. Kirschner, *J. Phys.: Condens. Matter* **3**: 4349 (1991)
9. P. Strange, J.B. Staunton, and H. Ebert, *Europhys. Lett.* **9**: 169 (1991)
10. F. Maca and J. Koukal, *Surf. Science* **260**: 323 (1992)
11. C.M. Schneider, J.J. de Miguel, P. Schuster, R. Miranda, B. Heinrich, and J. Kirschner, in: *Science and Technology of Nanostructured Magnetic Materials*, eds. G.C. Hadjippanayis and G.A. Prinz (Plenum Press, New York, 1991)
12. C. Liu, E.R. Moog, and S.D. Bader, *Phys. Rev. Lett.* **60**: 2422 (1988)
13. D. P. Pappas, K.-P. Kämper, and H. Hopster, *Phys. Rev. Lett.* **64**: 3179 (1990)
14. C.M. Schneider, J.J. de Miguel, P. Bressler, P. Schuster, R. Miranda, and J. Kirschner, *J. Electron Spec. Rel. Phen.* **51**: 263 (1990)
15. C.M. Schneider, D. Venus, and J. Kirschner, *Phys. Rev. B* **44**: 12066 (1991)
16. C. M. Schneider, P. Bressler, P. Schuster, J. Kirschner, J.J. de Miguel, R. Miranda and S. Ferrer, *Vacuum* **41**: 503 (1990)
17. H.P. Oepen, *J. Magn. Magn. Mat.* **93**: 116 (1991)
18. J. Goddard and J.G. Wright, *Br. J. Appl. Phys.* **16**: 1251 (1965)
19. B. Heinrich, J.F. Cochran, M. Kowalewski, J. Kirschner, Z. Celinski, A.S. Arrott, and K. Myrtle, *Phys. Rev. B* **44**: 9348 (1992)
20. C.M. Schneider, P. Bressler, P. Schuster, J. Kirschner, J.J. de Miguel, and R. Miranda, *Phys. Rev. Lett.* **64**: 1059 (1990)
21. M.T. Kief, G.J. Mankey, and R.F. Willis, *J. Appl. Phys.* **69**: 5000 (1991)
22. P. Bruno, in: "Magnetic Thin Films, Multilayers and Surfaces", Mat. Res. Soc. Symp. Proc. Vol. 231 (Materials Research Society, Pittsburgh, 1991)
23. J.J. de Miguel, A. Cebollada, J.M. Gallego, R. Miranda, C.M. Schneider, P. Schuster and J. Kirschner, *J. Magn. Magn. Mat.* **93**: 1 (1991)
24. A.K. Schmid and J. Kirschner, *Ultramicroscopy* (1992), in press
25. F. v.d. Merwe and E. Bauer, *Phys. Rev. B* **39**: 3632 (1989)
26. J. Frohn, M. Giesen, M. Poensgen, J.F. Wolf and H. Ibach, *Phys. Rev. Lett.* **67**: 3543 (1991)
27. A. Berger, U. Linke, and H.P. Oepen, *Phys. Rev. Lett.* **68**: 839 (1992)
28. H.P. Oepen, J. Kirschner, T. Reul, and C.M. Schneider, to be published
29. J. Chen and J.L. Erskine, *Phys. Rev. Lett.* **68**: 1212 (1992)
30. W.L. Egelhoff, jr. and M.T. Kief, *Phys. Rev. B* **45**: 7795 (1992)
31. R. Coehoorn et al., see these proceedings